physica status solidi b

phys. stat. sol. (b) **243**, No. 13, 3268–3272 (2006) / **DOI** 10.1002/pssb.200669176

Tube–tube interaction in double-wall carbon nanotubes

R. Pfeiffer[*, 1], **F. Simon**[1, 2], **H. Kuzmany**[1], **V. N. Popov**[3], **V. Zólyomi**[1, 4], and **J. Kürti**[5]

[1] Fakultät für Physik der Universität Wien, Strudlhofgasse 4, 1090 Wien, Austria
[2] Department of Experimental Physics, Budapest University of Technology and Economics, 1521 Budapest, Hungary
[3] Faculty of Physics, University of Sofia, Sofia, Bulgaria
[4] Research Institute for Solid State Physics and Optics of the Hungarian Academy of Sciences, P.O. Box 49, 1525 Budapest, Hungary
[5] Department of Biological Physics, Eötvös University, Pázmány Péter sétány 1/A, 1117 Budapest, Hungary

Received 21 April 2006, revised 2 June 2006, accepted 16 August 2006
Published online 26 September 2006

PACS 63.20.Dj, 78.30.Na, 78.66.Tr, 78.67.Ch

In a Raman map of double-wall carbon nanotubes, the radial breathing modes of the inner tubes are grouped into clusters with similar resonance behavior. These clusters are located close to the resonances of SDS wrapped HiPco tubes and can spread over 30 cm^{-1}. Compared to the HiPco tubes the resonances of the inner tubes are shifted about 50 meV to the red. Each cluster represents one fixed inner tube type in several different outer tube types and each component of a cluster originates from a well defined inner/outer tube pair. Elaborate inter-shell interaction models showed an increasing charge transfer from the outer to inner tube with decreasing diameter difference. Additionally, many DWCNTs systems seem to be metallic, i.e. they have a finite density of states at the Fermi level.

1 Introduction

Recently, much research was dedicated to double-wall carbon nanotubes (DWCNTs), especially to DWCNTs grown by high-vacuum annealing of (C_{60}) peapod precursors [1, 2]. The outer tubes of such DWCNTs have typical diameters of 1.4 nm. Considering the inter-shell spacing, the inner tubes have typical diameters of 0.7 nm. The small diameters of the inner tubes result in high curvatures and significant deviations from graphene with respect to the mechanical and electronic properties.

The Raman spectra of the radial breathing mode (RBM) region of DWCNTs show a much larger number of inner tubes RBMs than there are geometrically possible tubes [3–5]. Recording a Raman map of the DWCNT RBM region – i.e. a contour plot of the Raman intensity as a function of laser energy and RBM frequency – revealed that the inner tubes RBMs are grouped into clusters [5]. A comparison with a Kataura plot, calculated with an extended tight-binding method [6], of HiPco tubes dispersed in SDS [7–9] showed that the clusters are near the transitions of the HiPco tubes with a small red-shift of about 50 meV. [5] The clusters start around the HiPco frequencies and can extend up to 30 cm^{-1} to higher frequencies. Additionally, the clusters can consist of more than 10 well resolved components.

In this contribution, we concentrate on the consequences of the inter-shell interaction between inner and outer tubes and on the evaluation of the inner/outer tube pairs. For this we will focus on the clusters of the (6, 5) and (6, 4) inner tubes. Additionally, simulations suggest that charge is transferred from the outer to the inner tube and that many DWCNT systems have a finite density of states at the Fermi level.

[*] Corresponding author: e-mail: rudolf.pfeiffer@univie.ac.at, Phone: +43 1 4277 51378, Fax: +43 1 4277 51375

2 Experimental

The studied DWCNTs were grown by annealing C_{60} peapods at 1250 °C in a dynamic vacuum for 2 hours. The outer tubes had a mean diameter of 1.45 nm. The Raman spectra were measured with a Dilor xy triple grating spectrometer using the 568 nm (2.18 eV) line of an Ar/Kr laser and a dye laser with Rhodamine 6G as dye. The spectra were recorded at 80 K in high resolution mode. The frequency was calibrated with several calibration lamps from L.O.T.-Oriel. The Raman intensity was calibrated by the well known cross-section of the Si F_{1g} mode around 520 cm^{-1}.

3 Results

The upper part of Fig. 1 shows the high resolution RBM Raman response of the (6, 5) and (6, 4) inner tube clusters at 80 K for an excitation of 2.10 eV. For this excitation both clusters are close to their maximum intensity. The lower part of Fig. 1 shows the complete E_{22}^{S} Raman map of the (6, 5) and (6, 4) clusters. The green points are the corresponding transitions for the HiPco tubes. (The dashed lines denote the connections to next member of the respective families $2m + n = 17$ and $2m + n = 16$.)

The peaks between about 307 and 337 cm^{-1} were assigned to the (6, 5) cluster and the peaks between about 334 and 368 cm^{-1} were assigned to the (6, 4) cluster. Although the two clusters seem on a first glance to be well separated there is a small overlap. Especially, the very weak peak around 332 cm^{-1} was previously assigned to the (6, 4) cluster after comparing two DWCNTs samples with different mean outer tube diameters (Fig. 2 in Ref. [5]). Now it is assigned to the (6, 5) cluster. Nevertheless, the lowest frequencies of the clusters correspond roughly to the HiPco frequencies. The clusters of the (6, 5) and (6, 4) inner tubes consist of about 9 and of about 12 well resolvable components, respectively.

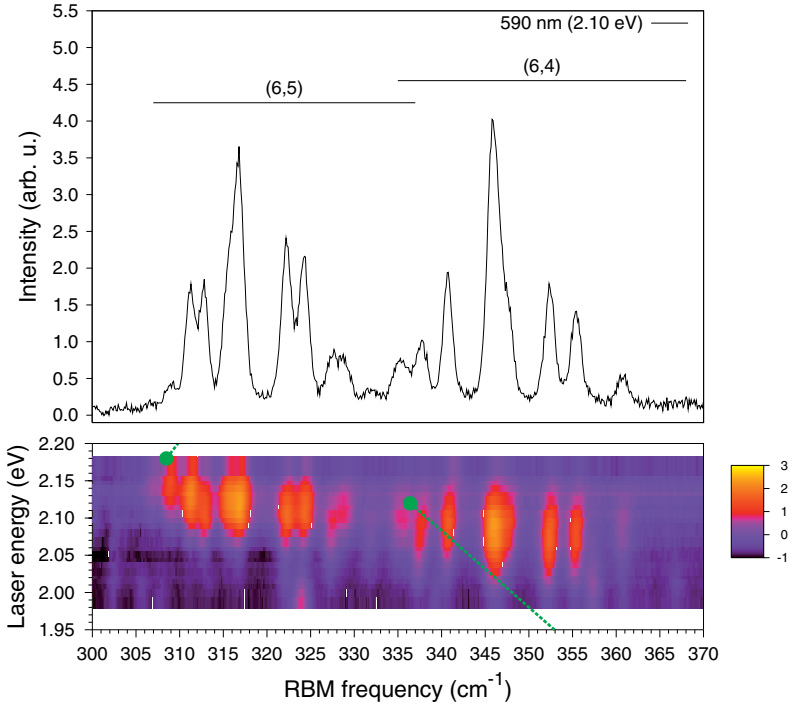

Fig. 1 (online colour at: www.pss-b.com) Top: High resolution RBM Raman response of the (6, 5) and (6, 4) clusters at 80 K for an excitation of 590 nm (2.10 eV). Bottom: E_{22}^{S} Raman map of the (6, 5) and (6, 4) clusters at 80 K. (Note that the logarithm of the Raman intensity is plotted.) The green points show the corresponding transitions in SDS wrapped HiPco tubes (averaged from Refs. [7–9]).

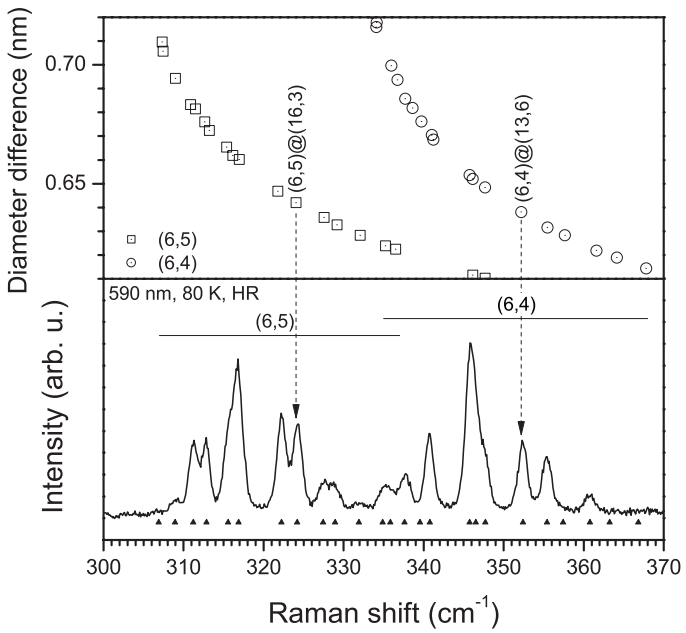

Fig. 2 Bottom: high resolution Raman response of the (6, 5) and (6, 4) inner tubes clusters for a 590 nm excitation. The triangles denote the measured frequencies obtained from fitting the spectrum with Voigtians. Top: RBM frequencies of the (6, 5) and (6, 4) inner tubes inside various outer tubes as calculated within the continuum model. The calculated frequencies were linearly scaled to fit the measured values. The dashed arrows show two explicit examples for assigning the individual RBM peaks to definite inner/outer tube pairs.

4 Discussion

4.1 Continuum model for the inter-shell interaction

The large number of inner tubes RBMs can be explained by assuming that one specific inner tube type can grow in several different outer tube types. When the diameter difference between inner and outer tube decreases the inter-shell interaction increases and the RBM of the inner tube shifts to higher frequencies, resulting in the components of the clusters in the DWCNTs Raman map. We calculated this frequency shift using a simple continuum model with two elastic cylinders coupled by a Lennard–Jones potential (parameterized for graphite) [4, 5]. The upper part of Fig. 2 shows this for the (6, 5) and (6, 4) inner tubes.

The triangles in the lower part of Fig. 2 depict the measured frequencies (see also Table 1). These were not obtained by just fitting the 590 nm spectrum but by fitting all spectra contributing to the Raman map in Fig. 1; i.e., small shoulders seen only in one or the other spectrum were not assigned an extra peak.

By comparing the calculated and measured frequencies one can now assign a definitive inner/outer tube pair to every single peak in the spectrum. This is explicitly shown for two examples in Fig. 2. The other inner/outer tube pairs are listed in Table. 1.

Table 1 summarizes the calculated RBM frequencies of the (6, 5) and (6, 4) inner tubes and shows the assignment to the measured frequencies. For large diameter differences the peaks of different inner/outer tube pairs are too close to each other to resolve them even in the high resolution spectra at low temperature. Additionally, the overlap of the two clusters between about 334 and 337 cm^{-1} prevents a definitive assignment in this region.

Table 1 RBM frequencies for the (6, 5) (left) and the (6, 4) (right) inner tube inside various outer tubes with chiralities (m, n) as calculated within the continuum model, $\omega_{\mathrm{RBM}}^{\mathrm{calc.}}$, and as measured, $\omega_{\mathrm{RBM}}^{\mathrm{exp.}}$. To obtain the points in the upper part of Fig. 2 the calculated frequencies of the two tubes were scaled with $0.84\omega_{\mathrm{RBM}}^{\mathrm{calc.}} + 45.3$ and $0.82\omega_{\mathrm{RBM}}^{\mathrm{calc.}} + 55.6$, respectively.

(m, n)	$\omega_{\mathrm{RBM}}^{\mathrm{calc.}}$	$\omega_{\mathrm{RBM}}^{\mathrm{exp.}}$
(12, 9)	318.16	311.23
(11, 10)	318.86	312.86
(17, 2)	321.40	315.58
(15, 5)	322.34	316.87
(18, 0)	323.28	
(14, 6)	329.03	322.26
(16, 3)	331.71	324.21
(13, 7)	335.93	327.43
(17, 1)	337.83	328.93
(12, 8)	341.29	331.90

(m, n)	$\omega_{\mathrm{RBM}}^{\mathrm{calc.}}$	$\omega_{\mathrm{RBM}}^{\mathrm{exp.}}$
(12, 8)	344.59	339.54n
(11, 9)	346.13	340.78
(15, 4)	346.13	
(10, 10)	346.39	
(16, 2)	351.88	345.74
(14, 5)	352.34	346.52
(17, 0)	354.23	347.71
(13, 6)	359.71	352.41
(15, 3)	363.67	355.43
(12, 7)	366.33	357.44
(11, 8)	371.10	360.77
(16, 1)	371.10	

4.2 More elaborate inter-shell interaction models

As described in Ref. [10], filling single-wall carbon nanotubes (SWCNTs) with ^{13}C enriched fullerenes can be used to grow DWCNTs with ^{12}C outer and ^{13}C inner tubes. This opened the possibility for NMR experiments on SWCNTs in the absence of other ^{13}C carbon phases. NMR studies [11] of these ^{13}C tubes suggested that many DWCNT systems are metallic.

In order to understand this result and to study the inter-shell interaction of DWCNTs over a wide range of inner and outer tube chiralities in more detail, we employed the inter-molecular Hückel model [12, 13] and DFT methods (VASP [14]) to calculate the electronic structures of the isolated inner and outer tubes and for the combined DWCNT [15, 16]. The band structure calculations showed that two semiconducting inner and outer tubes can yield a metallic DWCNT – in the sense of a finite density of states at the Fermi level – or at least a DWCNT with a band gap smaller than the individual tubes.

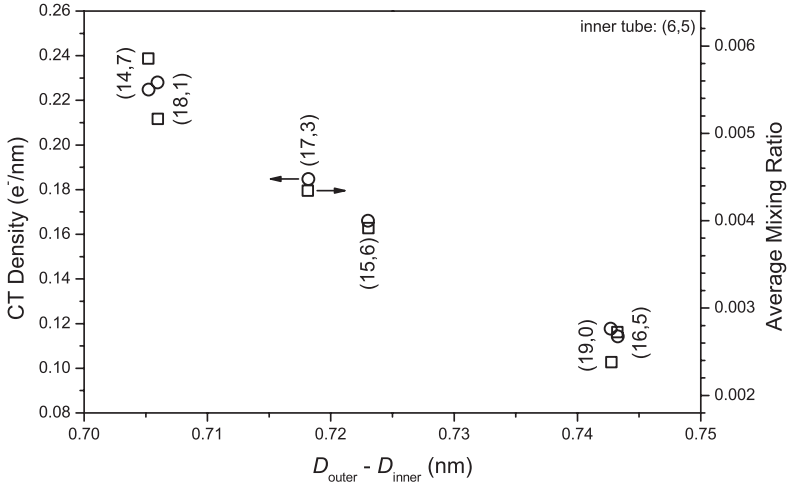

Fig. 3 Charge transfer from various outer tubes to a (6, 5) inner tube and orbital mixing between the outer tubes and a (6, 5) inner tube. The DWCNTs shown here were calculated using the IMH model.

When combining two individual SWCNTs into a DWCNT one has to consider two effects: (i) orbital mixing between the tubes, resulting in an overall compression of the band structure and (ii) charge transfer from the outer to the inner tube, which causes a shift of the Fermi level. Taking the (6, 5) inner tube as an example, Fig. 3 shows the charge transfer and the orbital mixing for several inner/outer tube pairs. In accordance with expectation, both the charge transfer and the orbital mixing increase with decreasing diameter difference.

5 Summary

In a Raman map of DWCNTs, the RBMs of the inner tubes are grouped into clusters where each cluster represents one fixed inner tube type in several different outer tube types. Each component of a cluster originates from a well defined inner/outer tube pair. This clustering of the inner tubes RBMs can be understood in a simple model of interacting elastic cylinders. More elaborate calculations of the inter-shell interaction revealed a charge transfer from the outer to the inner tube and suggest that most DWCNTs are metallic. The last point agrees with NMR experiments on DWCNTs with ^{13}C inner tubes.

Acknowledgements Valuable discussions with A. Jorio, A. Rubio and L. Wirtz are gratefully acknowledged. Work supported by FWF project P17345, Marie-Curie projects MEIF-CT-2003-501099 and MEIF-CT-2003-501080, by NATO CLG 980422, OTKA grants T038014 and K60576, and EU project NANOTEMP BIN2-2001-00580.

References

[1] B. W. Smith, M. Monthioux, and D. E. Luzzi, Nature **396**, 323–324 (1998).
[2] S. Bandow, M. Takizawa, K. Hirahara, M. Yudasaka, and S. Iijima, Chem. Phys. Lett. **337**, 48–54 (2001).
[3] R. Pfeiffer, H. Kuzmany, C. Kramberger, C. Schaman, T. Pichler, H. Kataura, Y. Achiba, J. Kürti, and V. Zólyomi, Phys. Rev. Lett. **90**, 225501 (2003).
[4] R. Pfeiffer, C. Kramberger, F. Simon, H. Kuzmany, V. N. Popov, and H. Kataura, Eur. Phys. J. B **42**, 345–350 (2004).
[5] R. Pfeiffer, F. Simon, H. Kuzmany, and V. N. Popov, Phys. Rev. B **72**, 161404(R) (2005).
[6] V. N. Popov, New J. Phys. **6**, 17 (2004).
[7] S. M. Bachilo, M. S. Strano, C. Kittrell, R. H. Hauge, R. E. Smalley, and R. B. Weisman, Science **298**, 2361–2366 (2002).
[8] C. Fantini, A. Jorio, M. Souza, M. S. Strano, M. S. Dresselhaus, and M. A. Pimenta, Phys. Rev. Lett. **93**, 147406 (2004).
[9] H. Telg, J. Maultzsch, S. Reich, F. Hennrich, and C. Thomsen, Phys. Rev. Lett. **93**, 177401 (2004).
[10] F. Simon, C. Kramberger, R. Pfeiffer, H. Kuzmany, V. Zólyomi, J. Kürti, P. M. Singer, and H. Alloul, Phys. Rev. Lett. **95**, 017401 (2005).
[11] P. M. Singer, P. Wzietek, H. Alloul, F. Simon, and H. Kuzmany, Phys. Rev. Lett. **95**, 236403 (2005).
[12] A. Lázár, P. Surján, M. Paulsson, and S. Stafström, Int. J. Quantum Chem. **84**, 216 (2002).
[13] P. Surján, A. Lázár, and Á. Szabados, Phys. Rev. A **68**, 062503 (2003).
[14] G. Kresse and J. Furthmüller, Phys. Rev. B **54**, 11169 (1996).
[15] V. Zólyomi, Á. Rusznyák, J. Kürti, Á. Gali, F. Simon, H. Kuzmany, Á. Szabados, and P. R. Surján, arXiv: cond-mat/0603407.
[16] V. Zólyomi, Á. Rusznák, J. Kürti, Á. Gali, F. Simon, H. Kuzmany, Á. Szabados, and P. R. Surján, phys. stat. sol. (b) **243**(13), (2006) (this issue).

